



Investigation of numerical and optimization method in the new concept of solar panel cooling under the variable condition using nanofluid

Abdulrahman A. Alrobaian¹ · Abdulrahman Saleh Alturki²

Received: 25 September 2019 / Accepted: 7 December 2019 / Published online: 4 January 2020
© Akadémiai Kiadó, Budapest, Hungary 2020

Abstract

Due to the warming of the earth and the increased cost of fossil fuel extraction, solar energy is a good alternative to power generation. Increasing the efficiency of solar systems such as photovoltaic panels has always been a matter of day in the field of industry and energy. In this research, using the genetic algorithm, we tried to optimize the hybrid cooling system. Then, considering the best model, we study the effect of the nanofluid in different volume fractions. The results show that the optimization model can increase about 13% more heat transfer. Also, the results showed that the use of nanosilver dioxide increases the heat transfer to the fluid. In this study, the thermal conductivity parameter for nanofluid is also considered as variable with temperature for a more precise examination of nanofluid properties.

Keywords Nanofluid · Optimization · Numerical method · Heat sink · Nusselt number

Introduction

Increasing pollution and decreasing conventional energies such as fossil fuels lead to seeking alternative energy resources. Among alternative energies, solar energy is a proper choice since eco-friendly and accessible. The chemical reactions that occur inside the sun at millions of degrees of temperatures generate energy and then dissipate into space [1]. Solar energy converts into electrical energy through the photovoltaic (PV) panels [2]. The solar panel includes several solar cells in series. All solar energy that reaches the surface of the PV panel cannot be converted into power and part of the energy is wasted. Heat energy losses lead to an increasing panel temperature and poor the performance of the system. The methods of efficiency enhancement in PV panels can be divided into two general groups: (1) active and (2) passive [3]. Much research has been carried out using design parameter optimization, active, and passive methods

to improve the efficiency of the PV panels, which are given in the following. The tilt angle is the main parameter, which influences the performance of the PV panel. Kaddoura et al. [4] determined the optimum tilt angle of the PV panel for some cities in Saudi Arabia by using the MATLAB code. The optimum tilt angle relies on the location of the sun and the geographic coordinates. The results showed that the optimum tilt angle varied monthly and seasonally. Xu et al. [5] determined the optimum tilt angle of a PV panel by considering the effect of dust. The dust caused an increase in the optimum tilt angle. Osma-Pinto and Ordóñez-Plata [6] carried out an experimental investigation on the impacts of kind of roof, installation height, and wind velocity on the efficiency of the PV panel. The results reveal that the efficiency enhancement was obtained on the green roof in the height range of 50 cm to 75 cm. Furthermore, an increase in wind velocity caused operating temperature reduction, which led to increasing the electrical efficiency of the PV panel. Abd-Elhady et al. [7] used Labovac oil, sunflower oil, and olive oil as coatings on the front surface of the silicon PV panel. They found that the PV panel with the Labovac oil coating had the highest efficiency due to the most transmissivity. An increase of about 20% was observed in the power output. Phase-change materials (PCMs) have a high capacity to absorb and store extra heat from the PV panel [8]. Stropnik and Stritih [9] performed an experimental and

✉ Abdulrahman A. Alrobaian
alrobaian@qu.edu.sa

¹ Department of Mechanical Engineering, College of Engineering, Qassim University, Buraydah, Saudi Arabia

² Department of Electrical Engineering, College of Engineering, Qassim University, Buraydah, Saudi Arabia

numerical investigation using TRNSYS software to study paraffin-type RT28HC effect on the efficiency of a PV panel model CS6P-M. The annual electrical energy generation enhanced 7.3% in comparison with the conventional PV panel. Rajvikram et al. [3] investigated the effect of PCM on the electrical efficiency of the PV panel. For this target, they used PCM that was covered by the aluminum sheet at the rear surface of the PV panel. The aluminum sheet was used to increase the thermal conductivity of the PCM. The PV panel efficiency increased by about 24.4%. Hemmer et al. [1] investigated the numerical simulation to study the heat transfer in PV panels. The tilt angle of the PV panel changed from to at solar radiation of 510 W m^{-2} in France. They found that the variation in the heat transfers in the PV panel had a weak dependence on the tilt angle. Furthermore, the maximum heat transfer rate was observed at the tilt angle. A three-dimensional analysis by using ANSYS software was conducted to study the heat transfer on the performance of the PV panel [2]. The optimum thickness of the spreader was 10 mm. The results indicate that they caused the decrease in cell temperature and the increase in efficiency up to about $20 \text{ }^\circ\text{C}$ and 10%, respectively. Fares et al. [3] used MATLAB optimization codes to achieve the optimal electrical quantities for a PV panel model ZT180S. Al-Waeli et al. [4] investigated the performance of the PV/T by using paraffin wax with nano-SiC under the panel and SiC/water nanofluid in the tank. They evaluated the system economically by using MATLAB software. The results reveal that the electrical efficiency of the PV/T increased by about 13.7% and the system was affordable. Abdallah et al. [5] assessed the performance of a PV/T system using Al_2O_3 /nanofluid as a working fluid. The maximum temperature reduction was about $8 \text{ }^\circ\text{C}$. Ebaid et al. [6] experimentally demonstrated that the performance of a PV panel with Al_2O_3 nanoparticles in the mixture of water and cetyltrimethylammonium bromide in the cooling system was better than TiO_2 nanoparticles in the mixture of water and polyethylene glycol. Sardarabadi et al. [5] experimentally examined the effect of using SiO_2 /water in the cooling system of the PV/T system in mass fraction percentage (mass%) of 1% and 3%. The maximum overall energy efficiency enhancement of the PV/T system was about 7.9% for SiO_2 /water at 3 mass%. Elmir et al. [7] simulated a PV/T system with Al_2O_3 /water as coolant. The heat transfer rate increased by about 27% when the nanoparticles concentration increased from 0 to 10%. Over time, research has focused on cooling solar panels from fin and heat sink to newer structures such as thermoelectric [8, 9] and PCM [10–12]. On the other hand, it is always optimized in this direction, and numerical methods are simultaneously advanced with the attempt to cool the photovoltaic panels. The use of optimization algorithms [38, 39] is also one of the things that is very much considered. In this study, by combining the optimization algorithm and the nanofluid

and the liquid cooling system, the first attempt was made to design an efficient cooling system in an environment with a temperature of $40 \text{ }^\circ\text{C}$ and a wind speed of 3 m s^{-1} .

Governing equation

The governing equations governing the flow of fluids for examination in the Cartesian coordinates in terms of fluid mechanics and heat transfer are presented for a constant fluid density and viscosity as follows. For the equation, we have continuity as [13]:

$$\frac{\partial}{\partial x_i} (\rho u_i) = 0 \quad (1)$$

Similarly, we will have a momentum equation [13]:

$$\frac{\partial (\rho u_i u_j)}{\partial x_j} = -\frac{\partial p}{\partial x_i} + \frac{\partial}{\partial x_j} \left[\mu \left(\frac{\partial u_i}{\partial x_j} + \frac{\partial u_j}{\partial x_i} \right) \right] - \frac{2}{3} \mu \frac{\partial u_k}{\partial x_k} \delta_{ij} \quad (2)$$

Energy equation [14]

$$\frac{\partial}{\partial x_i} \left(\rho u_i C_p T - k \frac{\partial T}{\partial x_j} \right) = u_j \frac{\partial p}{\partial x_j} + \left[\mu \left(\frac{\partial u_i}{\partial x_j} + \frac{\partial u_j}{\partial x_i} \right) \right] - \frac{2}{3} \mu \frac{\partial u_k}{\partial x_k} \delta_{ij} \quad (3)$$

Turbulence equations ($k - \epsilon$) RNG [15]

$$\begin{aligned} \frac{\partial}{\partial x_i} (\rho k u_i) &= \frac{\partial}{\partial x_j} \left[\left(\mu + \frac{\mu_j}{\sigma_k} \right) \frac{\partial k}{\partial x_j} \right] + G_k - \rho \epsilon \\ \frac{\partial}{\partial x_i} (\rho \epsilon u_i) &= \frac{\partial}{\partial x_j} \left[\left(\mu + \frac{\mu_t}{\sigma_k} \right) \frac{\partial \epsilon}{\partial x_j} \right] + C_{1\epsilon} \frac{\epsilon}{k} G_k - C_{2\epsilon} \rho \frac{\epsilon^2}{k} \end{aligned} \quad (4)$$

In the above relations, C_p is the specific heat of a constant volume, k is the kinetic energy of turbulence, $\hat{\mu}_t$ is the dispersion rate of turbulence, and the turbulence viscosity $\mu_t = \rho C_\mu \frac{K^2}{\epsilon}$, and p , T , u , v , and w represent the pressure, temperature, and the speed is along x , y and z .

Thermophysical properties of nanofluid

The following equation is used to obtain nanofluid densities [16]

$$(\rho)_{\text{nf}} = (1 - \varphi)\rho_f + \varphi\rho_p \quad (5)$$

The specific heat capacity of the nanofluid is calculated using the relationship provided by Rutzol and Zhouwan [17]

$$(C_p)_{\text{nf}} = \frac{(1 - \varphi)(\rho C_p)_f + \varphi(\rho C_p)_p}{\rho_{\text{nf}}} \quad (6)$$

In the above assumption, the thermal equilibrium between the base fluid and the nanoparticles is assumed. To calculate

the thermal conductivity coefficient of nanofluid which includes two static and dynamic sections, we used:

$$k_{nf} = k_{static} + k_{Brownian} \tag{7}$$

The static thermal conductivity coefficient is calculated from the following equation:

$$k_{static} = k_f \left[\frac{k_p + 2k_f - 2(k_f - k_p)\phi}{k_p + 2k_f + (k_f - k_p)\phi} \right] \tag{8}$$

The expression for the thermal conductivity of the inertia can also be calculated from the following equation [18, 19]

$$k_{Brownian} = 5 \times 10^4 \beta \phi \rho_f (C_p)_f \sqrt{\frac{K_b T}{\rho_p d_p}} f(T \cdot \phi) \tag{9}$$

In the above equation, d_p is equal to the diameter of the nanoparticles, $K_b = 1.3807 \times 10^{-23}$, Boltzmann constant, and β is the modeling function dependent on the concentration of nanoparticles, which is calculated using the following equation:

$$\beta = 8.4407(100\phi)^{-1.07304} \tag{10}$$

Problem description

This study is based on the need for cooling the solar panels in the warm areas. According to Fig. 1, a series of solar panels installed on a parking canopy was considered. The photovoltaic planes with specific dimensions were installed on the slopped part of the canopy. The proposed cooling system is schematically represented in Fig. 2. A heat sink with the fluid cooling agent was placed beneath the photovoltaic solar panel. A series of fins are also considered to increase the heat transfer surface

Figure 2 schematically illustrates the conventional methods used for cooling the photovoltaic panels. As this figure suggests, the heat produced as the result of solar radiation is usually transferred by a heat sink. Considering the heat sink condition, two general methods can be considered: porous heat sink and fluid cooling. The latter is proposed due to the possibility of using various cooling methods, and the third method was used in this study due to the nature of the problem and the temperature condition of the study area.

Investigation of the optimal condition for the network is a combination of the heat sink and cooling system. The schematic of geometric dimensions and boundary conditions is shown in Fig. 3. Different environmental conditions (including without wind and windy conditions with determined temperature) are listed in the boundary condition table in four designs. Any of these figures are then defined after an investigation by genetic algorithm and optimization in the form of the geometrical parameters as shown in Fig. 4. In

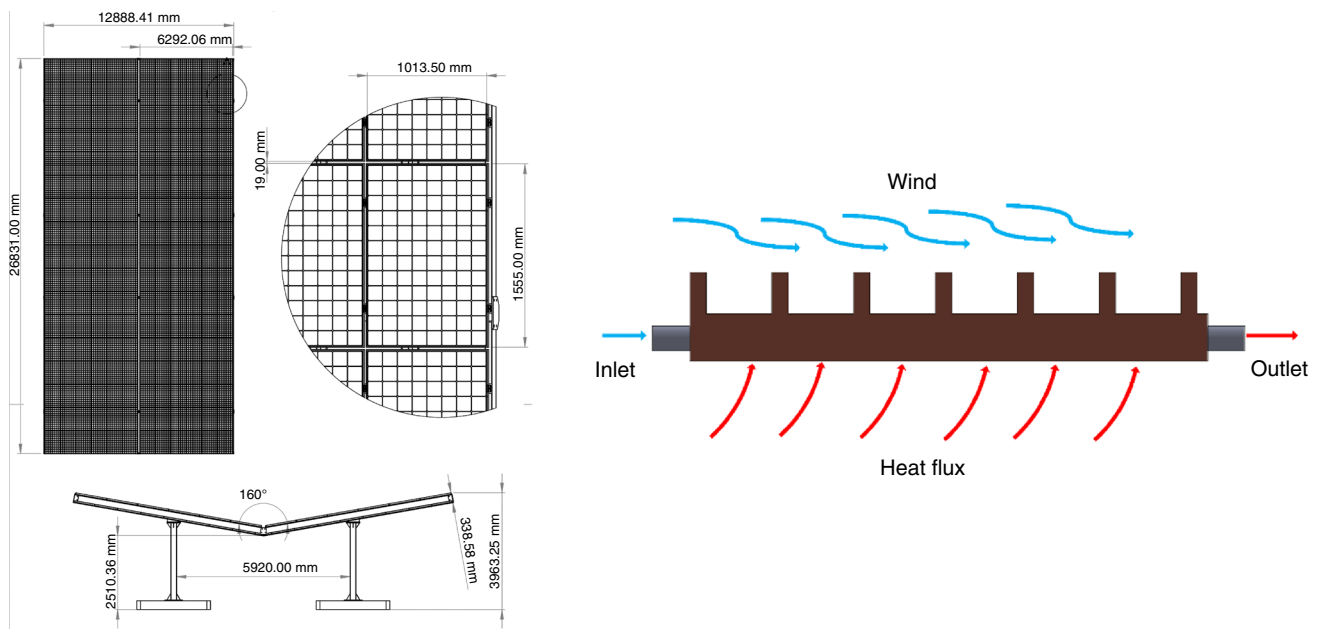


Figure 1 Problem and boundary conditions

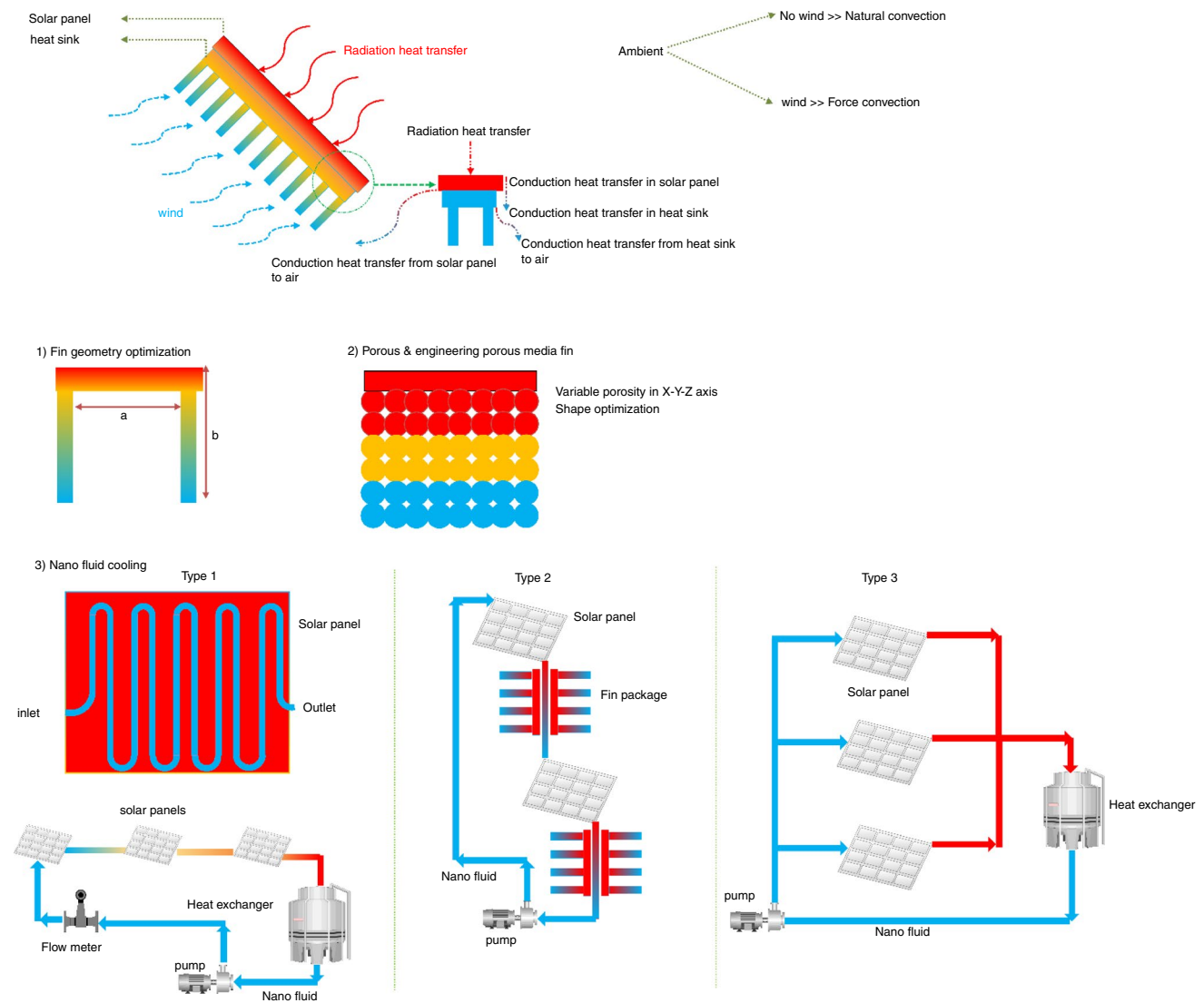


Figure 2 Different models of photovoltaic panel cooling with multiple cooling systems

other words, in this study, four models of fluid circulation in the heat sink were defined by the neural network whose properties are defined in Table 1. The optimal conditions were considered for evaluations.

To study environmental conditions on the efficiency of the cooling unit, two insights were considered. The first one (Table 1) was labeled as the geometrical optimization in which the genetic algorithm was employed to investigate four models with four different Re numbers covering the entire range of laminar to turbulent flows. The heat transfer and the effective variables on the thermal efficiency of the cooling unit were addressed. Then, by selecting the optimal condition from the four proposed ones, the effect of wind and nanofluids on increasing the heat transfer was evaluated. For this purpose, two nanofluids containing two volume fractions were compared with the base fluid (water); their

Nusselt number and heat distribution through the heat sink were investigated, and the boundary conditions and fluid characteristics for investigation of wind effect are listed in Table 2.

Validation

For each numerical method, the validation of the solved problem is of crucial importance. For this purpose, the obtained results were compared with the reference papers (Fig. 5) and the two conditions involving 850 and 1100 W m⁻² were validated. As shown in the Table 3, the maximum error for two aforementioned conditions of heat flux was 10.56%.

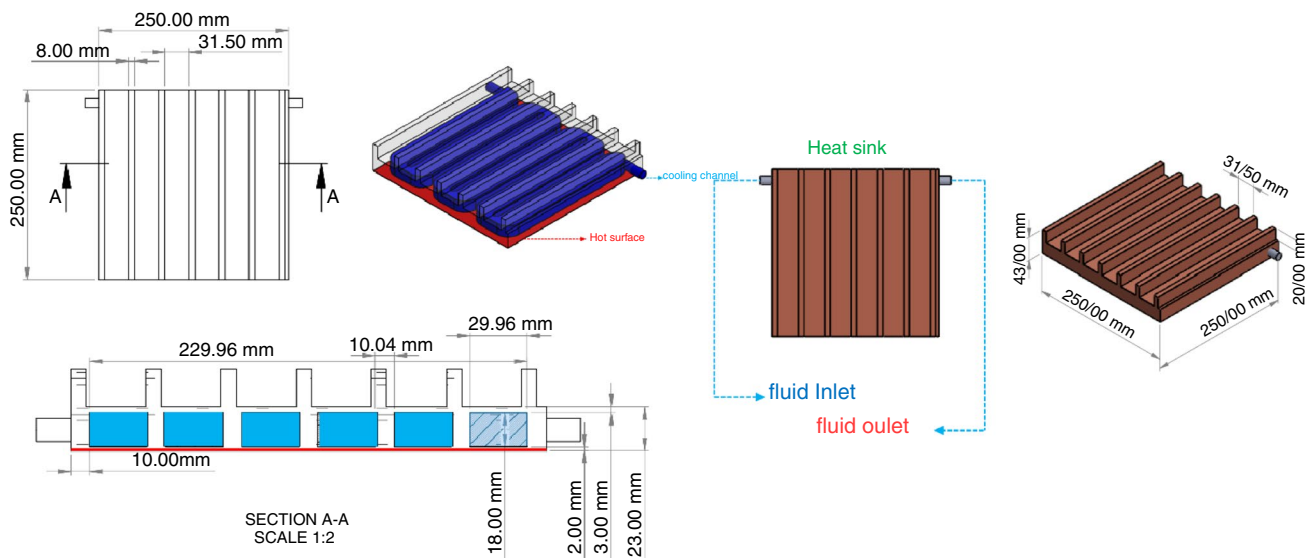


Figure 3 Geometric dimensions of the cooling system examined

Figure 4 Geometric dimensions of four proposed cooling systems

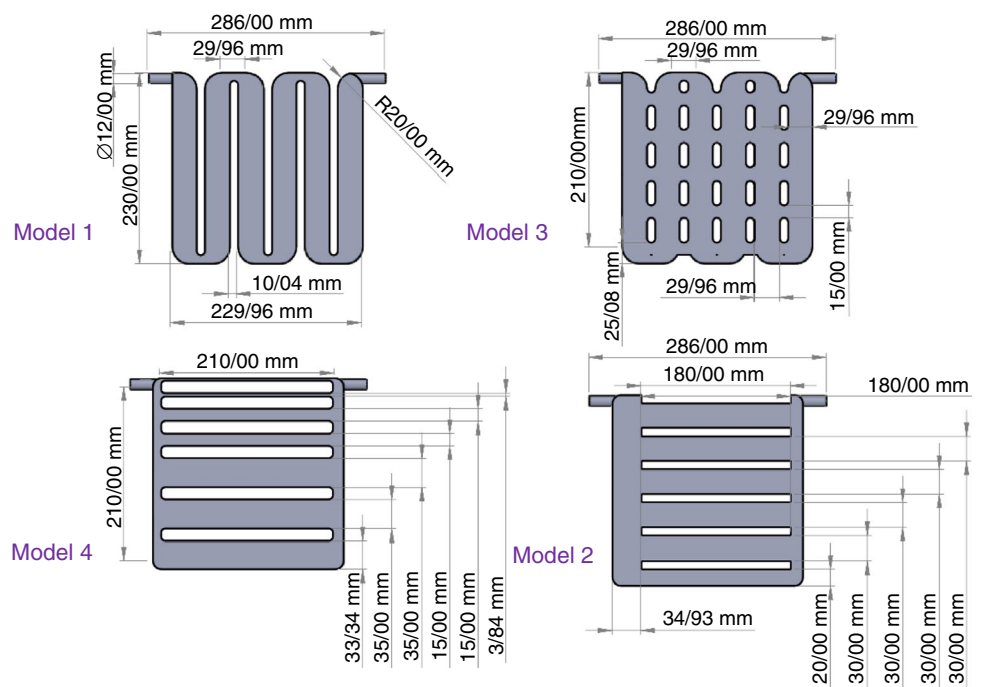


Table 1 Problem solving details with desired results

Type	Detail	No. of variable	Result
Geometry optimization	Four models	Four geometrical models	Temperature distribution
	Four Re numbers	Four Re numbers	Nu number
	No wind		Nu-Re plot
	Variable geometry		
Nanofluid	3 m s ⁻¹ direct wind	Two nanofluids	Temperature distribution
	Water and nanofluid compare	Two volume fractions	Nu number
	UDF thermal conductivity	Two Re numbers	Nu-Re plot

Table 2 Parameters calculation problem along with the initial conditions

Category		Model	Value			
			K	C_p	ρ	μ
Fluid	Cooling fluid	Water	0.6	4186	998.2	0.000853
		Al ₂ O ₃ (3%)	UDF	3820.80	1086.19	0.0012044
		Al ₂ O ₃ (4%)	UDF	3584.34	1115.92	0.0013203
		CuO (5%)	UDF	2963.28	8933	0.0010265
		CuO (3%)	UDF	3355.84	1235.18	0.0097444
	Wind	Air	0.0027	1.005	1.128	0.0000198
Solid	Aluminum		205	0.9	2700	–
Initial value	Inlet	Cooling fluid	Velocity inlet	Re = 6973		Re = 9962
		Wind	Velocity inlet	3 m s ⁻¹		
	Outlet	Cooling fluid	Pressure outlet	P0		
		Wind	Pressure outlet			
	Heat sink	Wall	Couple			
	Heat source	Wall	Heat flux			

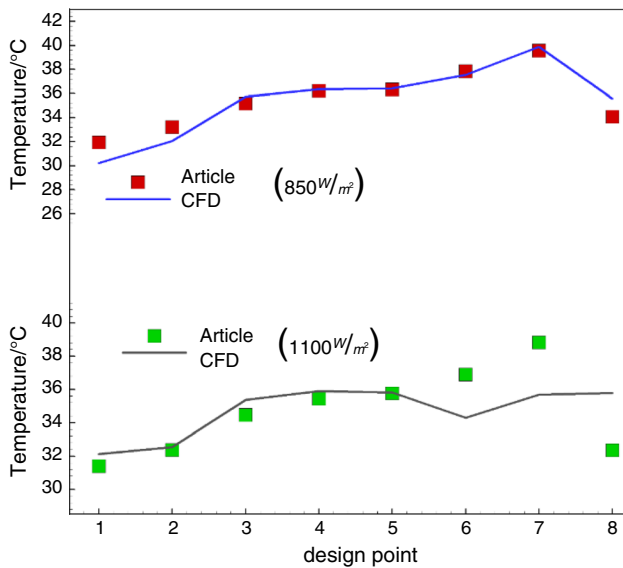


Figure 5 Validation of the temperature parameter for two modes with reference paper [20]

Mesh study and boundary conditions

In any numerical investigation, the study of the applied mesh is highly important in the parametric solution. As the calculations are conducted on the computational mesh, the accuracy of the mesh, as well as its parameters, should be investigated for each numerical study. According to the below figure, the mesh was investigated for all four states and the solution parameters were separately calculated and plotted for all the mesh formation states, and Fig. 6 indicates the independence of the mesh for all four models. The problem conditions, as well as the applied boundary conditions, are summarized in Table 4.

Moreover, the details of the problem solving along with the fluid models are presented. In this study, ICEM software was used for mesh generation on the models and ANSYS fluent was used as solver. MATLAB software was also used for geometrical optimization and optimization loop.

In Table 5, the solving details are observed for both geometric optimization and wind effects.

Table 3 Comparison of obtained values from numerical analysis and reference paper for different modes with error rate

Article (850 W m ⁻²)	Article (1100 W m ⁻²)	CFD (850 W m ⁻²)	CFD (100 W m ⁻²)	(%) (850 W m ⁻²)	(%) (1100 W m ⁻²)
31.94	31.40	30.21	32.12	5.422903178	-2.29
33.22	32.37	32.04	32.54	3.53	-0.53
35.16	34.46	35.741	35.39	-1.62	-2.62
36.22	35.43	36.3535	35.87	-0.34	-1.28
36.33	35.76	36.41	35.81	-0.20	-0.12
37.83	36.89	37.54	34.28	0.78	7.06
39.56	38.81	39.88	35.69	-0.80	8.07
34.07	32.36	35.57	35.78	-4.39	-10.56

Figure 6 Independence graphs of the grid for all four geometry states examined

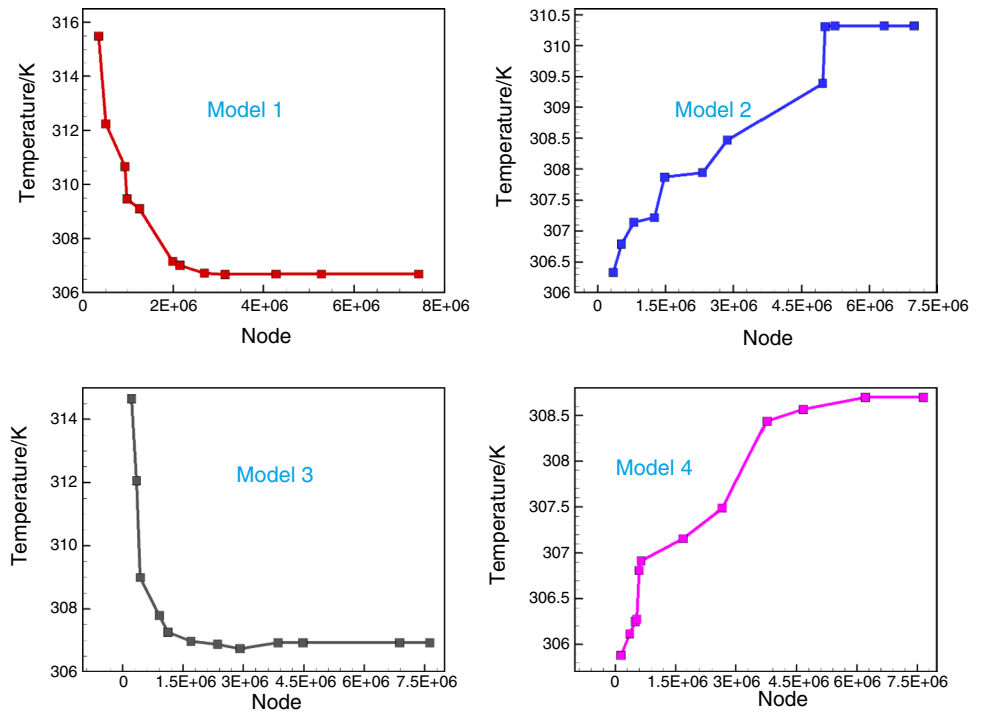


Table 4 Boundary condition

Parameter	Type	Calculation value	Unit
Heat flux	Radiation	1000	W m ⁻²
Temperature	Wall temperature	40.50	°C
Wind speed at 3 m	Outside wall	3	m s ⁻¹
Material	Fluid	Fe ₂ O ₃	4% volume fraction
		Al ₂ O ₃	3% volume fraction
	Solid	Copper	—
Velocity inlet	Laminar to turbulence range at inlet	Re=996	—
		Re=2989	—
		Re=6973	—
		Re=9962	—

Geometrical optimization

This study employed the genetic algorithm for geometrical optimization based on the Nusselt number. Figure 7 shows the optimization based on the response surface methodology (RSM) method [21–23]. For each geometry, the geometrical optimization parameters are defined in ten separate states. For the numerical analysis, the mesh production process and validation were also conducted as shown in the figure. In this optimization, the objective function was maximum Nusselt number and lowest pressure drop.

Results and discussion

Cooling of the photovoltaic panels will prolong their lifetime and increase their efficiency. Furthermore, regarding the radiation and temperature conditions of the studied area, cooling of the electricity production panels is of crucial importance. In general, as mentioned in Introduction section, the cooling methods are divided into natural and force convection. In the natural convection, heat sink, phase transition materials, and fins are important. Regarding the high temperature of the study area, the application of these

Table 5 Solving details

Variable	Model	Value
Viscous model	Geometrical optimization	Laminar for low Re Turbulent for high Re
		Laminar $K - \epsilon$ $v^2 - f$
Discretization	Wind	Turbulent
	Geometrical optimization	SIMPLE
	Wind	SIMPLEC
Fluid inlet	Geometrical optimization	Couple
		Velocity inlet
		Re = 996
		Re = 2989
	Wind	Re = 6973
		Re = 9962
		Velocity inlet
		3 m s ⁻¹
		Fluid
		Velocity inlet
Fluid outlet	Geometrical optimization	Pressure outlet
	Wind	Pressure outlet
Heat source		Heat flux
Heat sink		Coupled
		1000 W/m ²
		-

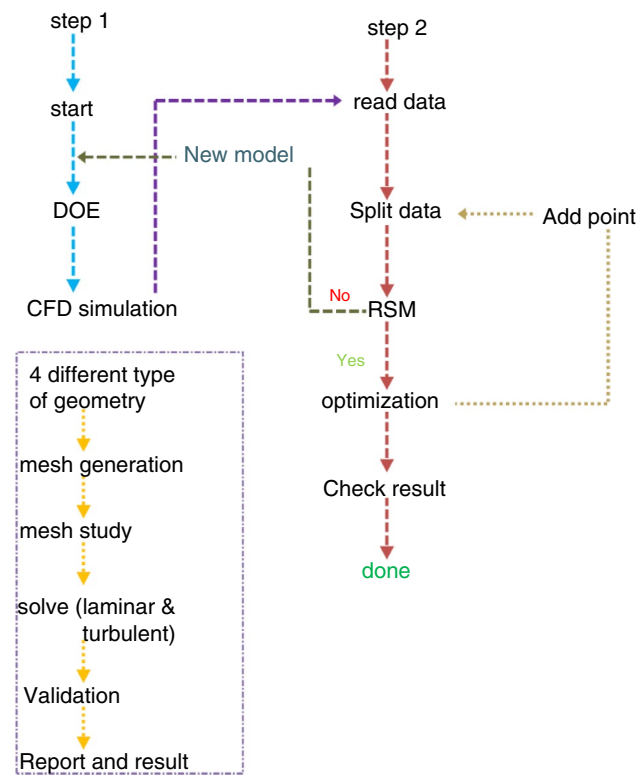


Figure 7 Geometric optimization algorithm by considering RSM method

methods cannot result in proper cooling. Blowing and fluid cooling are among the force convection. In this research, a combination of the natural and force convection was applied to enhance the cooling of the solar panel. The creation of fluid circulation tracts throughout the solar panel with the best fluid temperature distribution and lowest pressure drop was the reason for the application of the genetic algorithm in the cooling system. As shown in Fig. 3, the lower plane of the solar panel acted as the heat source with the maximum heat flux of 1000 W m⁻². Hybrid cooling system (fluid–heat sink) was precisely designed to increase the heat transfer. For instance, the minimum allowed a distance of the fluid system from the hot plate and standard distances from the sides, as well as the maximum possible fluid-hot plate contact area, were considered. The cold fluid flow starts to get hot by entering into the heat sink. The warming rate depends on the input fluid velocity, tract shape, and fluid properties. As the water was used as the fluid, the geometrical shape of the tract and the diffusion pattern are of crucial importance (Fig. 8) indicates the final results of the optimization algorithm for the tract geometry in four studied states. These results were obtained based on an analysis of 40 different geometrical shapes for each state. As depicted in Fig. 8 which shows the best state of each model, the fluid distribution in the cooling tracts significantly affected the thermal performance. It was also observed that the input Re could also influence the cooling performance. The fluid temperature distribution showed an apparent direct relationship with

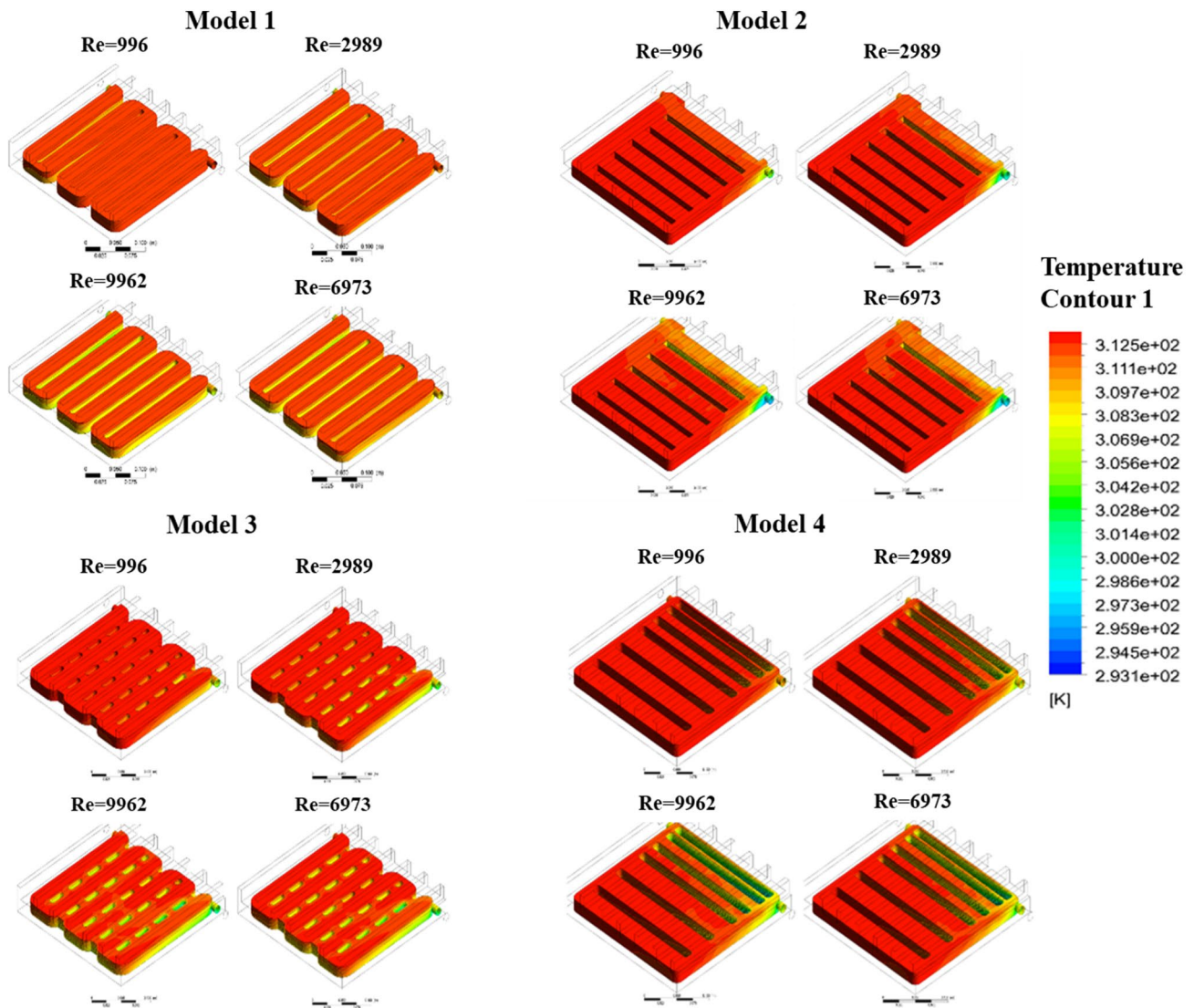


Figure 8 Distribution of temperature for the fluid zone in four models of cooling system

the velocity distribution. This can be further elucidated by investigation of the hot plane temperature distribution.

As shown in Fig. 9, models 1 and 3 showed more thermal uniformity compared to the other models. It was also indicated that for low input velocities, model 3 has more uniform temperature distribution. The important point in comparison with models 1 and 3 is that due to the high fluid velocity in model 1, temperature gradient increased by the Re number enhancement. This is not favorable for cooling. The optimal condition for a cooling system is the uniform reduction or increase in temperature throughout the fluid. Considering the mean fluid velocity in the cooling tract, model 3 will be a better choice for the cooling tract. The lower the slope of the line, the better the temperature distribution in the cooling track will be.

To compare the temperature distribution in the cooling tracts of all four proposed models, the dimensionless parameter of temperature uniformity is plotted versus the input Re in Fig. 10. Results showed that model 3 possessed a more uniform temperature distribution in comparison with other models. As mentioned before, uniform distribution of the temperature is a function of velocity distribution. The lower the velocity gradient in the tracts, the higher the temperature distribution and hence the heat transfer to the fluid will be. Table 6 lists the mean dimensionless velocity and temperature for various Re numbers for all four states. The results showed the highest velocity relative to the input velocity for model 3. The criterion for investigation of the heat transfer from the hot surface to the fluid at the temperature of 40 °C without consideration of wind is Nusselt number.

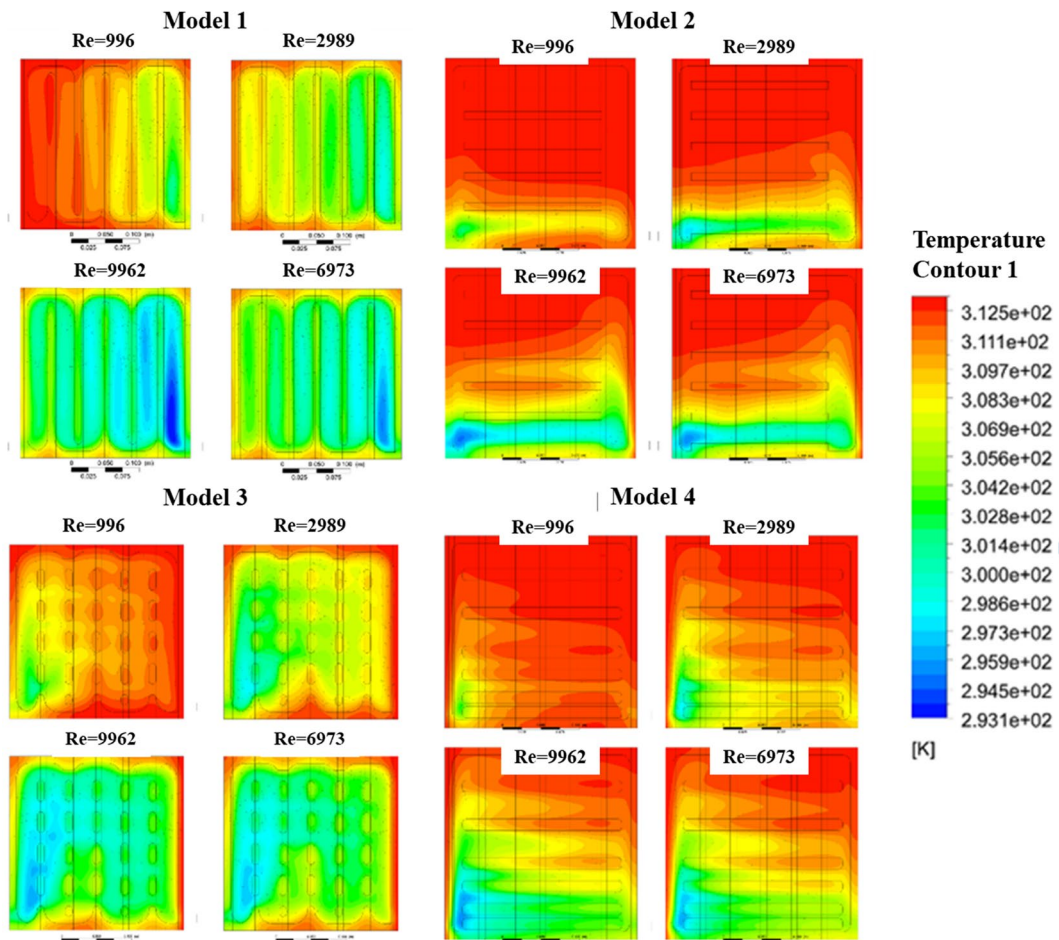


Figure 9 Temperature distribution for the plate connected to the photovoltaic panel

The Nusselt number is shown as a function of Re number for different Nu numbers in Fig. 10. Based on the results, model 3 had higher Re numbers. Furthermore, as expected, by an increase of Re number, the heat transfer rate increased as well. Regarding the boundary condition at 40 °C for the heat sink fins and absence of wind, the proposed model had

the highest Nusselt number according to its basic geometry. As mentioned before, the applied fluid is another effective parameter on the heat transfer. In the next section, by hanging the working fluid and boundary condition, the impacts of wind, nanofluid, and the volume fraction of the nanofluid (based on water) will be addressed (Figs. 11–15).

Figure 10 Non-dimensional temperature based on Reynolds number for various models of 1–4

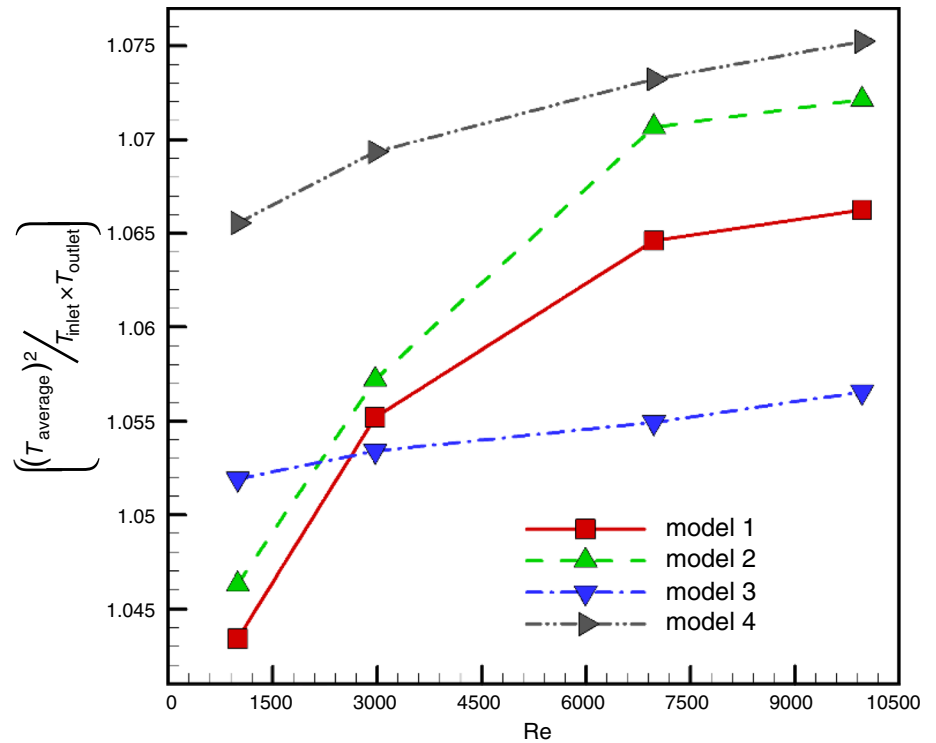


Table 6 Dimensionless velocity and temperature for various Re numbers

	Average temperature				Average velocity			
	Re = 996	Re = 2989	Re = 6973	Re = 9962	Re = 996	Re = 2989	Re = 6973	Re = 9962
Model 1	0.97	0.96	0.95	0.95	0.08	0.01	0.02	0.02
Model 2	0.99	0.98	0.98	0.98	0.01	0.03	0.06	0.06
Model 3	0.98	0.97	0.96	0.95	0.02	0.04	0.09	0.09
Model 4	0.98	0.97	0.97	0.97	0.02	0.03	0.06	0.07

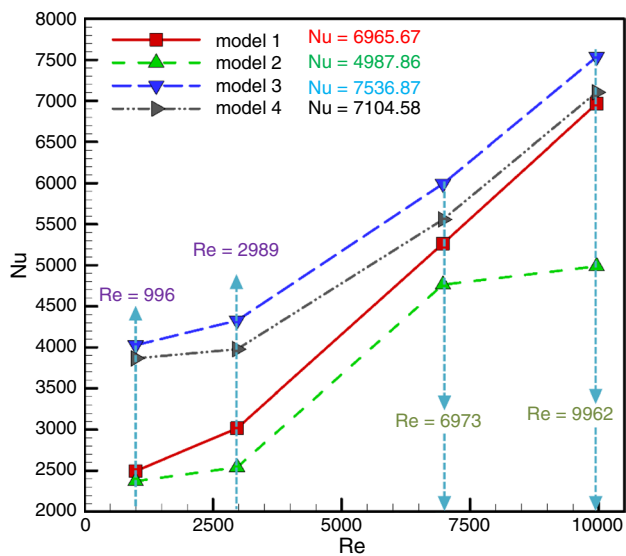


Figure 11 Nusselt number based on Reynolds number for various models of 1–4

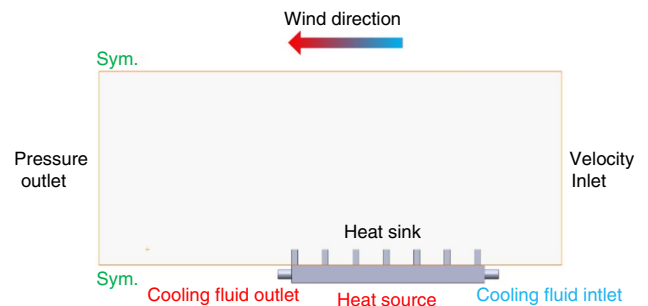


Figure 12 Graphic design of the boundary conditions used to model the wind around the cooling system

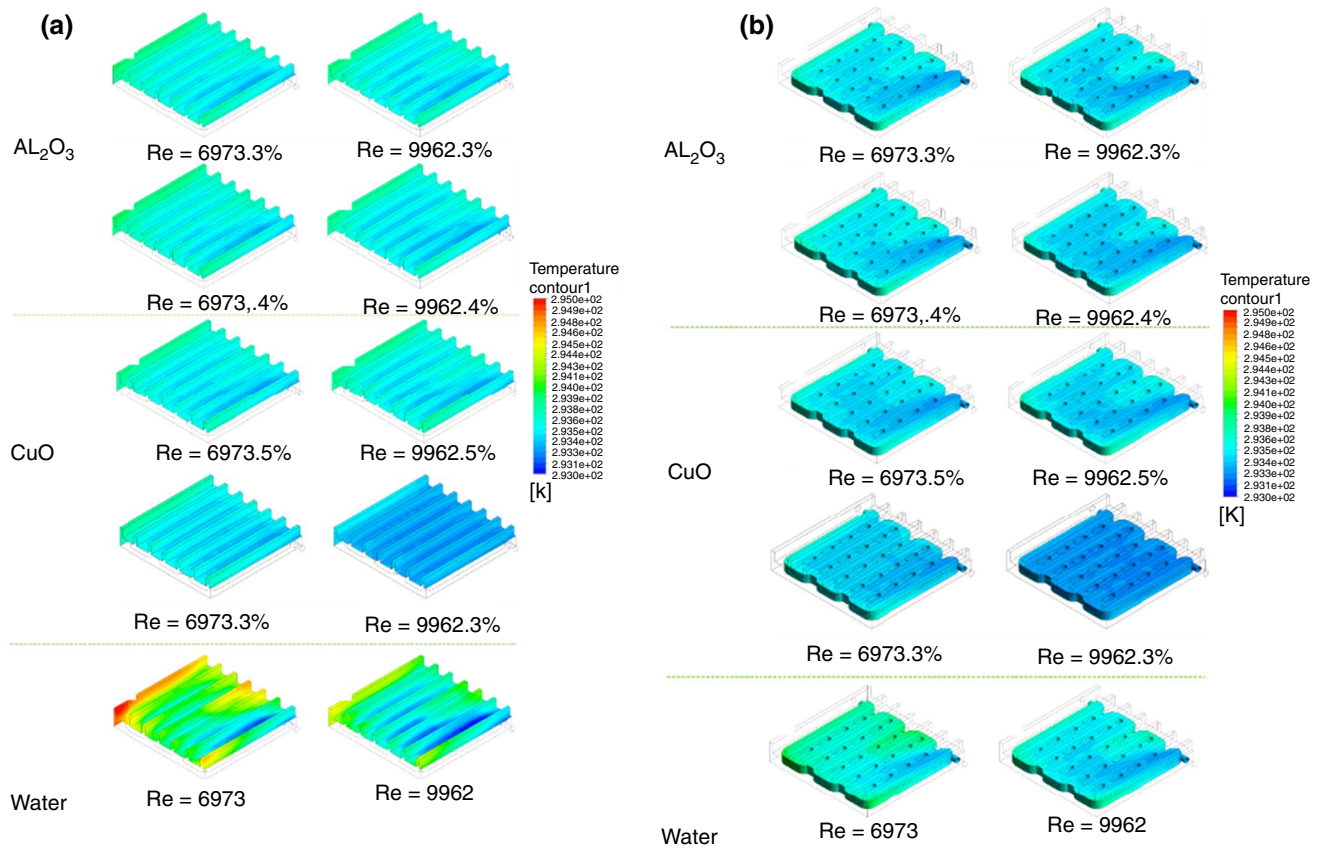


Figure 13 Temperature distribution for **a** heat sink, **b** coolant flow, and **c** heat absorber plate from photovoltaic panel for thermal flux 1000 W m^{-2}

Wind modeling

In the second part, the effect of nanofluid and its volume fraction (based on water) was investigated under windy conditions (3 m s^{-1}). The problem is schematically illustrated in Fig. 12. The wind flow was really modeled, and its effect on the surface was not only considered. The presence of airflow at $40 \text{ }^\circ\text{C}$ with a velocity of 3 m s^{-1} will affect the thermal regime of the cooling fluid. As the cooling fluid enters with a temperature of $20 \text{ }^\circ\text{C}$, the temperature distribution will be affected by the wind velocity and the environment temperature. The temperature repartition of the heat sink, hot

surface, and cooling tracts is shown in Fig. 13. The results are presented for aluminum oxide and copper oxide nanofluids for two volume fractions. As the effect of Re number was studied in the previous section, in this section, the Re of the turbulent part was investigated. The important point in this analysis is the consideration of the temperature-dependent nanofluid conductivity for all the nanofluids. As the thermal properties depend on the nanofluid temperature, by writing the properties code, the conductivity coefficient was considered for each volume fraction based on the temperature. According to the properties presented in Table 2, aluminum oxide and copper oxide were compared with water-based

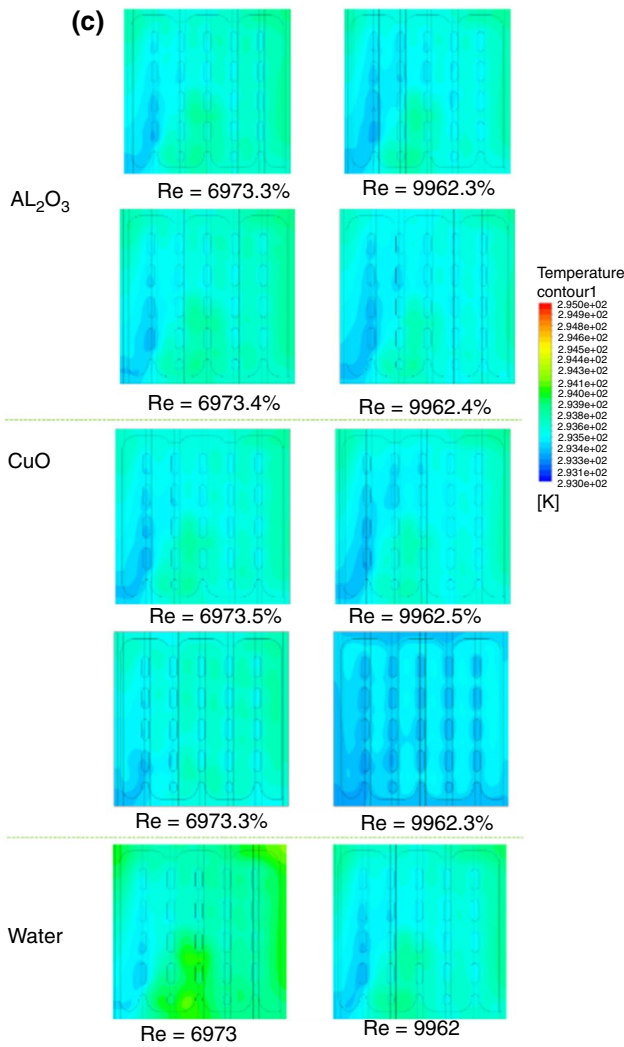


Figure 13 (continued)

fluid under similar boundary conditions. Contours in Fig. 13 show that the enhanced nanoparticles will enhance heat transfer. Moreover, the maximum temperature of the hot surface will be considerably decreased

As depicted in Fig. 13 a, the addition of nanofluid reduced the temperature of the heat sink fins. The conventional fluids used for heat transfer have low thermal conductivity; while the thermal conductivity of the metals is threefold higher; therefore, application of the solid metal particles and their combination with these fluids can increase the thermal conductivity and hence enhance the thermal efficiency. Figure 14a represents the temperature distribution in the cooling fluid as a dimensionless parameter. According to the results, the addition of nanofluid will enhance the temperature gradient of the cooling fluid throughout its path. In other words, by increasing the nanoparticle’s content, the fluid temperature difference will be higher in comparison with the water. Furthermore, 5 vol% of copper oxide induced higher heat transfer from the hot surface to the cooling fluid. This will be more evident by investigation of the heat sink temperature. Figure 14b shows the dimensionless temperature of the heat sink. Clearly, the application of nanofluid caused a higher gradient in comparison with the water. In a solar panel, the lower part experiences a constant heat flux.

Figure 15 presents the Nu number as a function of dimensionless length for two different Re numbers. Based on the results, an increase in the Re number increased the volume fraction from 3 to 5 vol%. Moreover, copper oxide nanofluid had a higher Nusselt number in both Re numbers.

Figure 14 Dimensionless number of temperature distribution for different nanofluids in fluid zone (a) and heat sink zone (b)

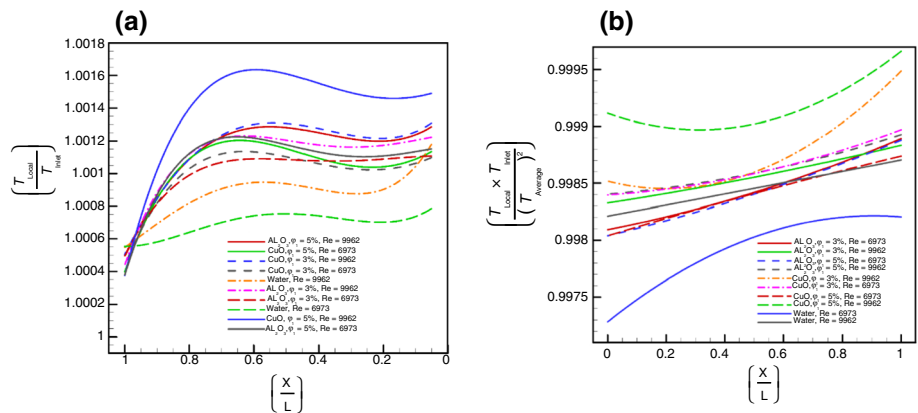
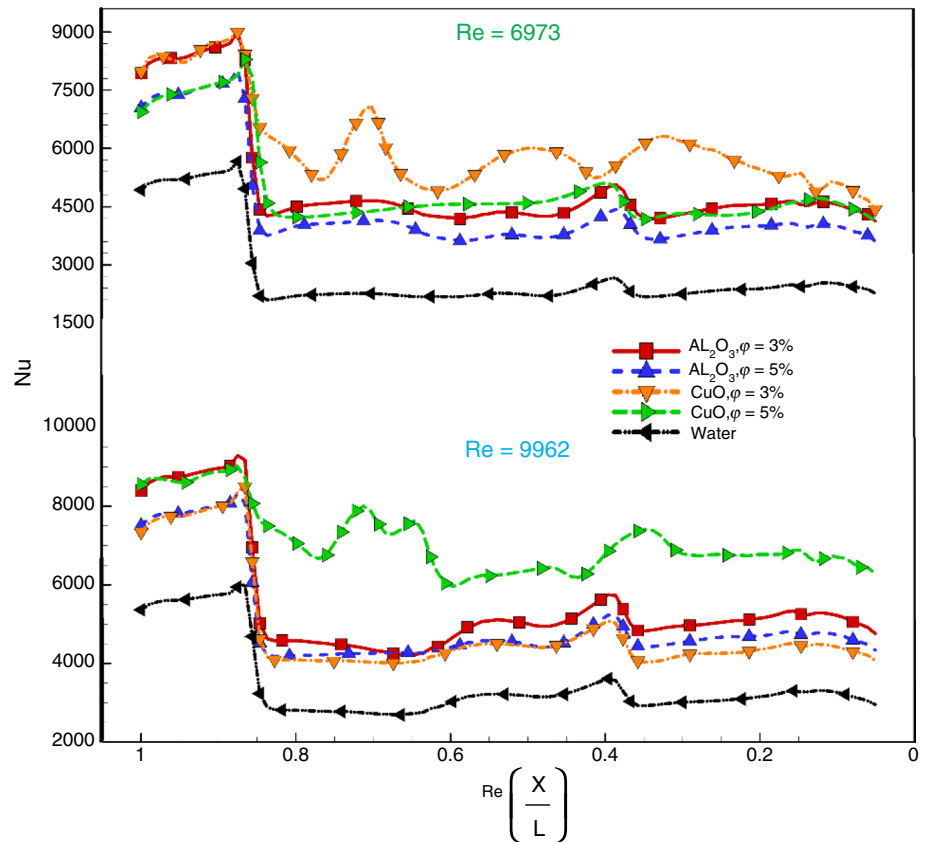


Figure 15 Nusselt number



Conclusions

In this study, using the optimization method for the internal structure of the cooling duct of the hybrid cooling system, we examined the optimum flow of intra-duct flow. In the next step, using a nanofluid, in a different volume fraction, we studied the variable and temperature properties effect on the nanofluid. In this study, RSM method is used for optimization. The result has shown that using the RSM method to help optimize the genetic algorithm improves the thermal efficiency of the fluid cooling network.

1. Based on the results of using the optimal method, the Nusselt number increases by 13% relative to the optimized model. Also, model 3 ultimately shows an 8% increase in Nusselt number compared to other models.
2. The results clearly revealed that the use of a fluid and heat sink combination network would cause more uniform temperature in the entire panel. Uniform temperature distribution causes no temperature gradient in the panel.
3. The results indicate that nanofluid copper oxide, with a volume fraction of 5%, causes the highest heat transfer rate.

4. Also, the results showed that by increasing Re number, the volume fraction of copper oxide is optimized from 3 to 5%. In other words, increasing Re number of flows, the volume fraction is 5% more Nusselt number
5. The result indicates that nanofluid can increase heat transfer in all type, but it recommended to use 5% of volume fraction in high Re number.
6. The result has shown that windy conditions cannot be used as a cooling parameter. The concept of cooling with optimizing geometry and nanofluid can provide reliable and constant PV temperature.

Acknowledgements The authors would like to thank Deanship of Scientific Research at Qassim University for supporting this work under Project Number 3980-qec-2018-1-14-S.

References

1. Hemmer C, et al. Early development of unsteady convective laminar flow in an inclined channel using CFD: application to PV panels. *Sol Energy*. 2017;146:221–9.
2. Soliman AM, et al. A 3d model of the effect of using heat spreader on the performance of photovoltaic panel (PV). *Math Comput Simul*. 2018;167:78–91.

3. Rafiei A, Alsagri AS, Mahadzir S, Loni R, Najafi G, Kasaeian A. Thermal analysis of a hybrid solar desalination system using various shapes of cavity receiver: cubical, cylindrical, and hemispherical. *Energy Convers Manag.* 2019;15(198):111861.
4. Al-Waeli AH, et al. Experimental investigation of using nano-PCM/nanofluid on a photovoltaic thermal system (PVT): technical and economic study. *Thermal Sci Eng Prog.* 2019;11:213–30.
5. Abdallah SR, et al. Experimental investigation on the effect of using nano fluid (Al_2O_3 -Water) on the performance of PV/T system. *Thermal Sci Eng Prog.* 2018;7:1–7.
6. Ebaid MS, Ghrair AM, Al-Busoul M. Experimental investigation of cooling photovoltaic (PV) panels using (TiO_2) nanofluid in water-polyethylene glycol mixture and (Al_2O_3) nanofluid in water-cetyltrimethylammonium bromide mixture. *Energy Convers Manag.* 2018;155:324–43.
7. Elmira M, Mehdaoui R, Mojtabi A. Numerical simulation of cooling a solar cell by forced convection in the presence of a nanofluid. *Energy Procedia.* 2012;18:594–603.
8. Dimri N, Tiwari A, Tiwari G. Effect of thermoelectric cooler (TEC) integrated at the base of opaque photovoltaic (PV) module to enhance an overall electrical efficiency. *Sol Energy.* 2018;166:159–70.
9. Shatar NM, et al. Design of photovoltaic–thermoelectric generator (PV-TEG) hybrid system for precision agriculture. In: 2018 IEEE 7th international conference on power and energy (PECon). 2018. IEEE.
10. Kabeel AE, El-Agouz SA. Review of researches and developments on solar stills. *Desalination.* In Press, Corrected Proof.
11. Rajvikram M, et al. Experimental investigation on the abasement of operating temperature in solar photovoltaic panel using PCM and aluminium. *Sol Energy.* 2019;188:327–38.
12. Setoodeh N, Rahimi R, Ameri A. Modeling and determination of heat transfer coefficient in a basin solar still using CFD. *Desalination.* 2011;268(1–3):103–10.
13. Cengel YA. *Fluid mechanics.* London: Tata McGraw-Hill Education; 2010.
14. Janna WS. *Introduction to fluid mechanics.* 1993: PWS-KENT.
15. Pope SB. *Turbulent flows.* Bristol: IOP Publishing; 2001.
16. Abu-Nada E, Chamkha AJ. Effect of nanofluid variable properties on natural convection in enclosures filled with a CuO–EG–water nanofluid. *Int J Therm Sci.* 2010;49(12):2339–52.
17. Li Q, Xuan Y, Wang J. Investigation on convective heat transfer and flow features of nanofluids. *J Heat Transfer.* 2003;125(2):151–5.
18. Karimipour A, et al. A new correlation for estimating the thermal conductivity and dynamic viscosity of CuO/liquid paraffin nanofluid using neural network method. *Int Commun Heat Mass Transfer.* 2018;92:90–9.
19. Zhu D, et al. Dispersion behavior and thermal conductivity characteristics of Al_2O_3 - H_2O nanofluids. *Curr Appl Phys.* 2009;9(1):131–9.
20. Yang D, et al. Simulation and experimental validation of heat transfer in a novel hybrid solar panel. *Int J Heat Mass Transf.* 2012;55(4):1076–82.
21. Anderson MJ, Whitcomb PJ. *RSM simplified: optimizing processes using response surface methods for design of experiments.* Abingdon: Productivity Press; 2016.
22. Bezerra MA, et al. Response surface methodology (RSM) as a tool for optimization in analytical chemistry. *Talanta.* 2008;76(5):965–77.
23. Han H-Z, et al. Multi-objective shape optimization of double pipe heat exchanger with inner corrugated tube using RSM method. *Int J Therm Sci.* 2015;90:173–86.

Publisher's Note Springer Nature remains neutral with regard to jurisdictional claims in published maps and institutional affiliations.